Weierstrass Institute for
Applied Analysis and Stochastics

Optimal control of multifrequency induction hardening

Dietmar Hömberg
joint work with Thomas Petzold (WIAS) and Elisabetta Rocca (Universita' degli Studi di Milano)

Content

What is induction hardening

- Induction hardening is a classical method for heat treatment of steel
- Procedure: Well-directed heating by electromagnetic waves and subsequent quenching of the surface

What is induction hardening

- Induction hardening is a classical method for heat treatment of steel
- Procedure: Well-directed heating by electromagnetic waves and subsequent quenching of the surface

- Induction hardening is a classical method for heat treatment of steel
- Procedure: Well-directed heating by electromagnetic waves and subsequent quenching of the surface

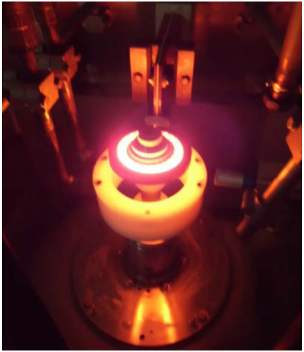

- Induction hardening is a classical method for heat treatment of steel
- Procedure: Well-directed heating by electromagnetic waves and subsequent quenching of the surface

Advantage: Very fast and energy-efficient process

Drawback: Difficult to generate desired close to contour hardening profile for complex work pieces such as gears

New approach: Multi-frequency induction hardening

- Simultaneous supply of medium- and high frequency power on one induction coil
- Close to contour hardening profile for gears and other complex-shaped parts

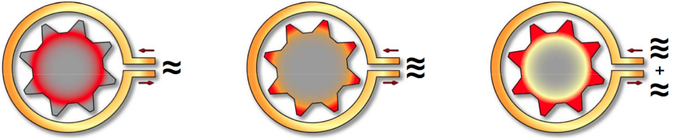

MF: nur der Zahnfuß wird erwärmt | HF: nur der Zahnkopf wird erwärmt | MF + HF: Zahnkopf und Zahnfuß werden erwärmt

MF | HF | MF + HF

The Me-Fre-Sim Consortium

- Weierstraß – Institut Berlin
- A. Schmidt, Universität Bremen (ZeTeM)
- R.W.H. Hoppe, Universität Augsburg (LAM)
- F. Hoffmann, IWT Bremen
- EFD Induction GmbH
- ZF Friedrichshafen AG

supported by BMBF program "Mathematics for innovations in industry and services"

Aims:

- Simulation of the process to reduce costly experiments
- Optimization of the process (Computation of optimal process parameters)

Three effects:

- Heat transfer
- Heat source Joule heating *(Maxwell's equations)*
- Phase transformations

- Maxwell's equations

$$\operatorname{curl} \boldsymbol{E} = -\frac{\partial \boldsymbol{B}}{\partial t}$$
$$\operatorname{div} \boldsymbol{B} = 0$$
$$\operatorname{curl} \boldsymbol{H} = \boldsymbol{J} + \frac{\partial \boldsymbol{D}}{\partial t}$$
$$\operatorname{div} \boldsymbol{D} = \rho$$

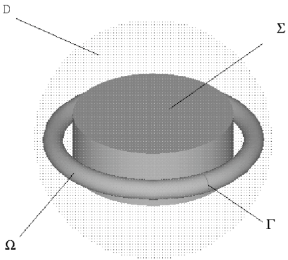

- Material equations

$$\boldsymbol{D} = \varepsilon \boldsymbol{E} \qquad \boldsymbol{B} = \mu \boldsymbol{H} \qquad \boldsymbol{J} = \sigma \boldsymbol{E}$$

$\boldsymbol{H}$	magnetic field	$\boldsymbol{B}$	magnetic induction
$\boldsymbol{E}$	electric field	$\boldsymbol{D}$	electric displacement field
$\boldsymbol{J}$	current density	ρ	charge density
σ, μ, ε	electric conductivity, magnetic permeability, electric permittivity		

- Magnetic vector potential $\boldsymbol{A}$
$$\boldsymbol{B} = \operatorname{curl} \boldsymbol{A}$$
- Electric scalar potential ϕ
$$\boldsymbol{E} = -\operatorname{grad}\phi - \frac{\partial \boldsymbol{A}}{\partial t}$$
- Neglecting the electric displacement ($|\partial \boldsymbol{D}/\partial t| \ll |\boldsymbol{J}|$)
$$\begin{aligned} \sigma \frac{\partial \boldsymbol{A}}{\partial t} + \operatorname{curl} \frac{1}{\mu} \operatorname{curl} \boldsymbol{A} + \sigma \operatorname{grad}\phi &= 0 \quad \text{on} \quad D \\ -\operatorname{div} \sigma \operatorname{grad}\phi &= 0 \quad \text{on} \quad \Omega \end{aligned}$$
- Potential $\boldsymbol{A}$ is not unique, gauging condition necessary ($\operatorname{div} \boldsymbol{A} = 0$)

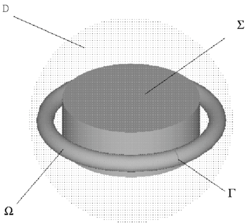

- Introduction of boundary conditions on ∂D
  1. Perfect electric conductor $\boldsymbol{E} \times n = 0$
  2. Perfect magnetic conductor $\boldsymbol{H} \times n = 0$

(1) leads to

$$\boldsymbol{A} \times \boldsymbol{n} = 0$$

(2) leads to

$$\mu^{-1} \operatorname{curl} \boldsymbol{A} \times \boldsymbol{n} = 0$$

- Conditions for the scalar potential

$$\sigma \operatorname{grad} \phi \cdot \boldsymbol{n} = 0 \quad \text{on} \quad \partial\Omega$$

$$[\![\sigma \operatorname{grad} \phi \cdot \boldsymbol{n}]\!] = 0 \quad \text{and} \quad [\![\phi]\!] = U_0 \quad \text{on} \quad \Gamma$$

- For a given coil geometry (here a torus with rectangular cross-section), the source current density $\boldsymbol{J} = \sigma \operatorname{grad} \phi$ can be precomputed analytically
- From $\operatorname{div} \sigma \operatorname{grad} \phi = 0$ one obtains in cylindrical coordinates

$$\phi = C_1 \varphi \quad \text{and consequently} \quad \boldsymbol{J} = \sigma C_1 \, (0, 1/r, 0)^T_{(r,\varphi,z)}$$

where $C_1 = U_0/(2\pi)$ for a given voltage

Eliminating the scalar potential

- For a given coil geometry (here a torus with rectangular cross-section), the source current density $\boldsymbol{J} = \sigma \operatorname{grad} \phi$ can be precomputed analytically
- From $\operatorname{div} \sigma \operatorname{grad} \phi = 0$ one obtains in cylindrical coordinates

$$\phi = C_1 \varphi \quad \text{and consequently} \quad \boldsymbol{J} = \sigma C_1 \left(0, 1/r, 0\right)^T_{(r,\varphi,z)}$$

  where $C_1 = U_0/(2\pi)$ for a given voltage
- For a given source current in the coil C_1 is computed from

$$\int_\Gamma \boldsymbol{J} \cdot \boldsymbol{n} \,\mathrm{d}a = I_{\text{coil}}$$

- In cartesian coordinates one obtains for a given source current

$$\boldsymbol{J} = \frac{I_{\text{coil}}}{\log(r_A/r_I)h} \begin{pmatrix} -y/(x^2+y^2) \\ x/(x^2+y^2) \\ 0 \end{pmatrix}$$

- Rate laws relate phase fraction z and temperature θ

z_0	ferrite,
	pearlite,
	martensite
$z_0(t_0) = 1$	

Phase fractions

- Rate laws relate phase fraction z and temperature θ

z_0	ferrite, pearlite, martensite
$z_0(t_0) = 1$	

$\xrightarrow{\text{heating}}$

z_0	initial composition
z_1	austenite
$z_0 + z_1 = 1$	

Phase fractions

- Rate laws relate phase fraction z and temperature θ

z_0	ferrite, pearlite, martensite

$z_0(t_0) = 1$

$\xrightarrow{\text{heating}}$

z_0	initial composition
z_1	austenite

$z_0 + z_1 = 1$

$\xrightarrow{\text{cooling}}$

z_0	initial composition
z_1	austenite
z_2	ferrite
z_3	pearlite
z_4	martensite

$\sum z_i = 1$

Phase fractions

- Rate laws relate phase fraction z and temperature θ

z_0	ferrite, pearlite, martensite

$z_0(t_0) = 1$

$\xrightarrow{\text{heating}}$

z_0	initial composition
z_1	austenite

$z_0 + z_1 = 1$

$\xrightarrow{\text{cooling}}$

z_0	initial composition
z_1	austenite
z_2	ferrite
z_3	pearlite
z_4	martensite

$\sum z_i = 1$

- Rate equations for phase fraction of austenite $z := z_1$

$$\dot{z}(t) = f(\theta, z) = [z_{\text{eq}}(\theta) - z]_+ g(\theta)$$
$$z(0) = 0$$

- Model consists of vector-potential formulation of Maxwell's equation, heat equation and rate law for phase fractions
- Source term $\boldsymbol{J}$ can be used as control for optimization

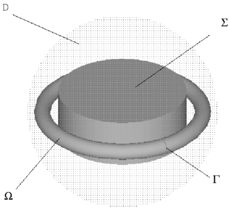

$$\sigma \frac{\partial \boldsymbol{A}}{\partial t} + \operatorname{curl} \frac{1}{\mu} \operatorname{curl} \boldsymbol{A} = \boldsymbol{J} \qquad \text{on } D$$

$$c_p \rho \frac{\partial \theta}{\partial t} - \operatorname{div} \kappa \operatorname{grad} \theta = \sigma \left| \frac{\partial \boldsymbol{A}}{\partial t} \right|^2 - \rho L \frac{\partial z}{\partial t} \qquad \text{in } \Sigma$$

$$\dot{z}(t) = [z_{\text{eq}}(\theta) - z]_+ g(\theta) \qquad \text{in } \Sigma$$

$$z(0) = 0$$

where

$$\boldsymbol{J} = u(t)\boldsymbol{J}_0 \quad \text{and} \quad \boldsymbol{J}_0 = \left(-y/(x^2+y^2), x/(x^2+y^2), 0\right)^T$$

Analysis and control of Joule heating models – a few references

- Resistance heating
  - heat source $h = \sigma|\nabla\varphi|^2, \quad \longrightarrow$ thermistor problem
  - Cimatti, Prodi (1988); Howison, Rodrigues, Shillor (1993); Antonsev Chipot (1994), H., Khludnev, Sokolowski (2001); H., Meyer, Rehberg (2010)

- Resistance heating
  - heat source $h = \sigma|\nabla\varphi|^2, \quad \longrightarrow$ thermistor problem
  - Cimatti, Prodi (1988); Howison, Rodrigues, Shillor (1993); Antonsev Chipot (1994), H., Khludnev, Sokolowski (2001); H., Meyer, Rehberg (2010)
- Induction heating – time domain heat source $h = \sigma(\theta)|\nabla\varphi + A_t|^2$
  - Bossavit, Rodrigues (1994); H., Sokolowski (2003); H. (2004),

Analysis and control of Joule heating models – a few references

- Resistance heating
  - heat source $h = \sigma|\nabla\varphi|^2, \quad \longrightarrow$ thermistor problem
  - Cimatti, Prodi (1988); Howison, Rodrigues, Shillor (1993); Antonsev Chipot (1994), H., Khludnev, Sokolowski (2001); H., Meyer, Rehberg (2010)
- Induction heating – time domain heat source $h = \sigma(\theta)|\nabla\varphi + A_t|^2$
  - Bossavit, Rodrigues (1994); H., Sokolowski (2003); H. (2004),
- Induction heating – frequency domain
  - F. Bachinger, U. Langer, J. Schöberl: *Numerical analysis of nonlinear multiharmonic eddy current problems*. Numer. Math. **100**(2005)
  - Druet, Klein, Sprekels, Tröltzsch, Yousept: *Optimal control of 3D state-constrained induction heating problems with nonlocal radiation effects* SICON **49** (2011)
  - Tröltzsch, F.; Yousept, I.: *PDE–constrained optimization of time-dependent 3D electromagnetic induction heating by alternating voltages*. ESAIM: M2AN **46** (2012)

- Constitutive assumptions

$$\sigma(x,z) = \begin{cases} 0, & x \in D \setminus G\,, \\ \sigma_w(z), & x \in \Sigma\,, \\ \sigma_i, & x \in \Omega\,, \end{cases} \qquad \mu(x,z) = \begin{cases} \mu_0, & x \in D \setminus G\,, \\ \mu_w(z), & x \in \Sigma\,, \\ \mu_i, & x \in \Omega\,, \end{cases}$$

- solution space for vector potential
  $\mathbf{X} = \left\{ v \in \mathbf{L}^2(D) \,\middle|\, \operatorname{curl} v \in \mathbf{L}^2(D)\,,\ \operatorname{div} v = 0\,, n \times v\big|_{\partial D} = 0 \right\}$
- assume $\partial D \in C^{1,1}$ then $\mathbf{X}$, equipped with the norm

$$\|v\|_{\mathbf{X}} = \|\operatorname{curl} v\|_{\mathbf{L}^2(D)}\,,$$

  is a closed subspace of $\mathbf{H}^1(D)$
- regularity of initial and boundary conditions
  $g \in L^\infty(0,T; L^\infty(\partial\Sigma))$; $A_0 \in \mathbf{X} \cap \mathbf{H}^3(D)$, $\theta_0 \in W^{2,5/3}(\Sigma)$

(P): Find a triple (A, θ, z) satisfying

$$\int_G \sigma(x,z) A_t \cdot v \,\mathrm{d}x + \int_D \frac{1}{\mu(x,z)} \operatorname{curl} A \cdot \operatorname{curl} v \,\mathrm{d}x = \int_\Omega J_0(x) u(t) \cdot v \,\mathrm{d}x$$

for all $v \in \mathbf{X}$, a.e. in $(0,T)$,

$$\theta_t - \Delta\theta = -L(\theta, z) z_t + \sigma(x,z)|A_t|^2 \quad \text{a.e. in } Q \,,$$

$$z_t = \frac{1}{\tau(\theta)} \left(z_{eq}(\theta) - z\right)^+ \quad \text{a.e. in } Q \,,$$

$$\frac{\partial\theta}{\partial\nu} + \theta = g \quad \text{a.e. on } \partial\Sigma \times (0,T) \,,$$

$$A(0) = A_0, \quad \text{a.e. in } D, \quad \theta(0) = \theta_0, \quad z(0) = 0 \quad \text{a.e. in } \Sigma$$

Theorem 1:

(P) has a solution (A, θ, z) satisfying

$$\|A\|_{H^2(0,T;\mathbf{L}^2(D))\cap W^{1,\infty}(0,T;\mathbf{X})} + \|\operatorname{curl} A\|_{L^\infty(0,T;\mathbf{L}^6(D))}$$

$$+\|\theta\|_{W^{1,5/3}(0,T;L^{5/3}(\Sigma))\cap L^{5/3}(0,T;W^{2,5/3}(\Sigma))\cap L^2(0,T;H^1(\Sigma))\cap L^\infty(Q)}$$

$$+\|z\|_{W^{1,\infty}(0,T;W^{1,\infty}(\Sigma))} \leq S$$

where the the constant S depends on the data of the problem.

Theorem 2:

Let (A_i, θ_i, z_i) ($i = 1, 2$) be two triples of solutions corresponding to data $(A_{0,i}, \theta_{0,i}, u_i)$, then, there exists a positive constant $C = C(S)$ such that

$$
\begin{aligned}
&\|(A_1 - A_2)(t)\|^2_{\mathbf{L}^2(D)} + \|\operatorname{curl}(A_1 - A_2)\|^2_{\mathbf{L}^2(D\times(0,T))} \\
&\quad + \|\partial_t(A_1 - A_2)(t)\|^2_{\mathbf{L}^2(D)} + \|\operatorname{curl}(\partial_t(A_1 - A_2))\|^2_{\mathbf{L}^2(D\times(0,T))} \\
&\quad + \|(\theta_1 - \theta_2)(t)\|^2_{L^2(\Sigma)} + \|\theta_1 - \theta_2\|^2_{L^2(0,T;H^1(\Sigma))} \\
&\quad + \|(z_1 - z_2)(t)\|^2_{H^1(\Sigma)} + \|\partial_t(z_1 - z_2)\|^2_{L^2(0,T;H^1(\Sigma))} \\
&\le C\Big(\|A_{0,1} - A_{0,2}\|^2_{\mathbf{X}} + \|(\partial_t(A_1 - A_2))(0)\|^2_{\mathbf{L}^2(D)} + \|\theta_{0,1} - \theta_{0,2}\|^2_{L^2(\Sigma)} \\
&\qquad + \|u_1 - u_2\|^2_{H^1(0,T)}\Big) \quad \text{for all } t \in [0, T]\,.
\end{aligned}
$$

- cost functional

$$J(A,\theta,z;u) = \frac{\beta_1}{2}\int_0^T\int_\Sigma(\theta(x,t)-\theta_d(x,t))^2dxdt + \frac{\beta_2}{2}\int_\Sigma(z(x,T)-z_d)^2dx + \frac{\beta_3}{2}\|u\|^2_{H^1(0,T)}$$

- cost functional

$$J(A,\theta,z;u) = \frac{\beta_1}{2}\int_0^T\int_\Sigma(\theta(x,t)-\theta_d(x,t))^2\,dx\,dt + \frac{\beta_2}{2}\int_\Sigma(z(x,T)-z_d)^2\,dx + \frac{\beta_3}{2}\|u\|^2_{H^1(0,T)}$$

- control problem **(CP)**
  $\min J(A,\theta,z;u)$
  such that $A,\ \theta,\ z$ satisfies **(P)** and $u \in \mathcal{U}_{ad} \subset H^1(0,T)$

- cost functional

$$J(A,\theta,z;u) = \frac{\beta_1}{2}\int_0^T\int_\Sigma (\theta(x,t)-\theta_d(x,t))^2\,dx\,dt + \frac{\beta_2}{2}\int_\Sigma (z(x,T)-z_d)^2\,dx + \frac{\beta_3}{2}\|u\|^2_{H^1(0,T)}$$

- control problem **(CP)**
  $\min J(A,\theta,z;u)$
  such that $A,\ \theta,\ z$ satisfies **(P)** and $u \in \mathcal{U}_{ad} \subset H^1(0,T)$
- **Theorem:**
  (CP) has a solution $u \in \mathcal{U}_{ad}$

- adjoint system

$$
\begin{aligned}
-\sigma\alpha_t - \operatorname{curl}\left(\frac{1}{\mu}\operatorname{curl}\alpha\right) - \sigma'(x,z)z_t\alpha &= -2(\sigma A_t\vartheta)_t \\
-\vartheta_t - k\Delta\vartheta + f_\theta(\theta,z)\vartheta &= f_\theta\zeta + \beta_1(\theta-\theta_d) \\
-\zeta_t - f_z(\theta,z)\zeta + \sigma' A_t\cdot\alpha - \sigma'|A_t|^2\vartheta &= \frac{\mu'}{\mu^2}\operatorname{curl} A\cdot\operatorname{curl}\alpha - f_z\vartheta
\end{aligned}
$$

$$
\begin{aligned}
\alpha\times n &= 0 \quad \text{in } \partial D\times(0,T) \\
k\,\frac{\partial\vartheta}{\partial\nu} + \kappa\vartheta &= 0 \quad \text{in } \partial\Sigma\times(0,T) \\
\vartheta(T) &= 0\,,\ \zeta(T) = z(x,T) - z_d(x) \quad \text{in } \Sigma \\
\alpha(T) &= 0 \quad \text{in } D
\end{aligned}
$$

Optimal control problem – II

- adjoint system

$$
\begin{aligned}
-\sigma\alpha_t - \operatorname{curl}\left(\frac{1}{\mu}\operatorname{curl}\alpha\right) - \sigma'(x,z)z_t\alpha &= -2(\sigma A_t\vartheta)_t \\
-\vartheta_t - k\Delta\vartheta + f_\theta(\theta,z)\vartheta &= f_\theta\zeta + \beta_1(\theta-\theta_d) \\
-\zeta_t - f_z(\theta,z)\zeta + \sigma' A_t\cdot\alpha - \sigma'|A_t|^2\vartheta &= \frac{\mu'}{\mu^2}\operatorname{curl} A\cdot\operatorname{curl}\alpha - f_z\vartheta
\end{aligned}
$$

$$
\begin{aligned}
\alpha\times n &= 0 \quad \text{in } \partial D\times(0,T) \\
k\frac{\partial\vartheta}{\partial\nu} + \kappa\vartheta &= 0 \quad \text{in } \partial\Sigma\times(0,T) \\
\vartheta(T) &= 0,\ \zeta(T) = z(x,T) - z_d(x) \quad \text{in } \Sigma \\
\alpha(T) &= 0 \quad \text{in } D
\end{aligned}
$$

- variational inequality

$$
\int_0^T \Big(\beta_3\bar{u}(t) - \int_D \alpha(x,t)\cdot J(x,t)dx\Big)(u-\bar{u})dt
$$

$$
+\int_0^T \beta_3 u'(t)(u'(t)-\bar{u}'(t))dt \geq 0 \qquad \text{for all } u\in\mathcal{U}_{ad}\subset H^1(0,T)
$$

- Multiple time scales

  Magnetic vector potential and heat conductance live on different time scales

  (Averaging method)

Numerical simulation – challenges

- Multiple time scales

  Magnetic vector potential and heat conductance live on different time scales (Averaging method)

- Skin effect

  Eddy currents are distributed in a small surface layer of the workpiece (Adaptive mesh generation)

Numerical simulation – challenges

- Multiple time scales

  Magnetic vector potential and heat conductance live on different time scales (Averaging method)
- Skin effect

  Eddy currents are distributed in a small surface layer of the workpiece (Adaptive mesh generation)
- Nonlinear material data

  Magnetic permeability depends on temperature *and* magnetic field $\boldsymbol{H}$ (Linearization)

- Multiple time scales

  Magnetic vector potential and heat conductance live on different time scales (Averaging method)

- Skin effect

  Eddy currents are distributed in a small surface layer of the workpiece (Adaptive mesh generation)

- Nonlinear material data

  Magnetic permeability depends on temperature *and* magnetic field $\boldsymbol{H}$ (Linearization)

- (Dis-)Continuity of vector fields

  $\boldsymbol{A} \in H(\mathrm{curl})$ requires special class of finite elements (Nédélec elements)

- Multiple time scales

  Magnetic vector potential and heat conductance live on different time scales (Averaging method)
- Skin effect

  Eddy currents are distributed in a small surface layer of the workpiece (Adaptive mesh generation)
- Nonlinear material data

  Magnetic permeability depends on temperature *and* magnetic field $\boldsymbol{H}$ (Linearization)
- (Dis-)Continuity of vector fields

  $\boldsymbol{A} \in H(\mathrm{curl})$ requires special class of finite elements (Nédélec elements)
- 3D

  Time consuming simulation in 3D (Model reduction to tackle optimal control problem numerically)

- Time scale for Maxwell's equation governed by frequency of source current: $f \approx 10\ \mathrm{kHz} - 100\ \mathrm{kHz}$, consequetly $\tau \sim 10^{-5}\mathrm{s}$
- Time scale for heat equation governed by heat diffusion:

$$\tau \sim \frac{c_p \rho \mathsf{L}^2}{k} \approx 1\ \mathrm{s}$$

- Time scale for Maxwell's equation governed by frequency of source current: $f \approx 10\ \mathrm{kHz} - 100\ \mathrm{kHz}$, consequetly $\tau \sim 10^{-5}\mathrm{s}$
- Time scale for heat equation governed by heat diffusion:

$$\tau \sim \frac{c_p \rho \mathsf{L}^2}{k} \approx 1\ \mathrm{s}$$

- *Alternating computation:*
  - Solve for $\boldsymbol{A}$ with fixed temperature *on fast time-scale*
  - Compute Joule heat by averaging electric energy $Q = \frac{1}{T}\int_0^T \sigma \left|\frac{\partial \boldsymbol{A}}{\partial t}\right|^2 \mathrm{d}t$
  - Solve heat equation with fixed magnetic potential *on slow time-scale* (one time step)
  - Update $\boldsymbol{A}$ since σ and μ change with temperature

Skin effect

- Tendency of AC current to distribute near the surface of a conductor
- Current density decreases exponentially with growing depth
- Skin depth δ depends on frequency and material

$$\delta = \frac{1}{\sqrt{\pi f \mu \sigma}}$$

Skin effect

- Tendency of AC current to distribute near the surface of a conductor
- Current density decreases exponentially with growing depth
- Skin depth δ depends on frequency and material

$$\delta = \frac{1}{\sqrt{\pi f \mu \sigma}}$$

- Eddy current region must be resolved by computational grid
- Residual based error estimator allows adaptive grid refinement [Beck, Hiptmair, Hoppe, Wohlmuth 2000])

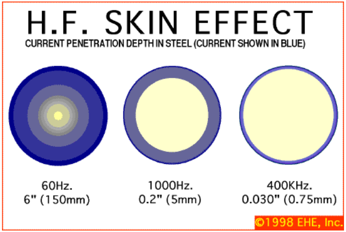

- Material data depend on temperature

  Electrical conductivity $\sigma(T)$

  Thermal conductivity $\kappa(T)$

  Density $\rho(T)$

  Specific heat capacity $c_p(T)$

- Nonlinear relation between magnetic induction $\boldsymbol{B}$ and magnetic field $\boldsymbol{H}$:

  Magnetization curve $\boldsymbol{B} = f(\theta, \boldsymbol{H}) = \mu(\theta, \boldsymbol{H})\boldsymbol{H}$

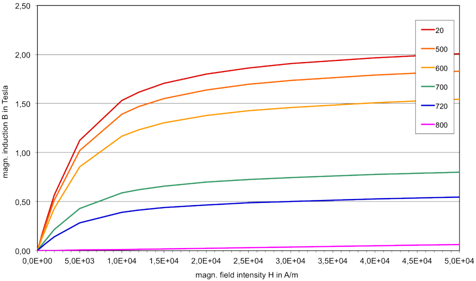

Nonlinear data: effective permeability

- Instead of solving the complete nonlinear system, we assume that only a time averaged value of the permeability affects the magnetic field

(i) Solve for the magnetic field with constant relative permeability $\hat{\mu}_r$

- Instead of solving the complete nonlinear system, we assume that only a time averaged value of the permeability affects the magnetic field

(i) Solve for the magnetic field with constant relative permeability $\hat{\mu}_r$

(ii) The magnetic field is periodic, this induces a periodic permeability

$$\mu(\theta(t,x), \boldsymbol{H}(x,t)) = \mu_0 \mu_{\mathrm{r}}(\theta(t,x), \boldsymbol{H}(x,t))$$

- Instead of solving the complete nonlinear system, we assume that only a time averaged value of the permeability affects the magnetic field

(i) Solve for the magnetic field with constant relative permeability $\hat{\mu}_r$

(ii) The magnetic field is periodic, this induces a periodic permeability

$$\mu(\theta(t,x),\boldsymbol{H}(x,t)) = \mu_0\mu_{\mathsf{r}}(\theta(t,x),\boldsymbol{H}(x,t))$$

(iii) Averaging over one period yields an effective permeability that depends on space, but is independent of the magnetic field. According to [Clain et al, 1992], a harmonic mean value performs best, i.e.,

$$\frac{1}{\mu_{\mathsf{r,av}}(x)} = \frac{1}{T}\int_0^T \frac{1}{\mu_{\mathsf{r}}(\theta(t,x),\boldsymbol{H}(x,t))}\,\mathrm{d}t$$

- Due to physical nature of magnetic and electric fields, $H(\mathrm{curl})$ is the natural vector space
- Less smoothness then H^1 (only tangential continuity)
- The triple $\{K, \mathcal{P}, \mathcal{N}\}$ denotes the *Nédélec element of 1st kind* with

$$K \subset \mathbb{R}^3 \quad \text{tetrahedron}$$

$$\mathcal{P} = \left\{ \boldsymbol{u} = \boldsymbol{a} + \boldsymbol{b} \times x \quad \forall\, \boldsymbol{a}, \boldsymbol{b} \in \mathbb{R}^3 \right\}$$

$$\mathcal{N} = \left\{ M_e \,:\, M_e(\boldsymbol{u}) = \int_e \boldsymbol{u} \cdot \boldsymbol{t} \,\mathrm{d}l \quad \forall\, e \text{ edges of } K, \forall \boldsymbol{u} \in \mathbb{R}^3 \right\}$$

  K element domain, $\mathcal{P}$ polynomial space, $\mathcal{N}$ degrees of freedom
- There holds

$$P^0(K) \subset \mathcal{P} \subset P^1(K) \quad \text{and} \quad \mathrm{curl}\, \mathcal{P} = P^0(K)$$

- Non-trivial large kernel of the curl-operator challenging for iterative solution of discretized Maxwell problems

  $\longrightarrow$ suitable preconditioner for Maxwell's equation required

Example 1

- Disc heated with HF and MF
- Adaptive grid
- Austenite profile
- Temperature profile

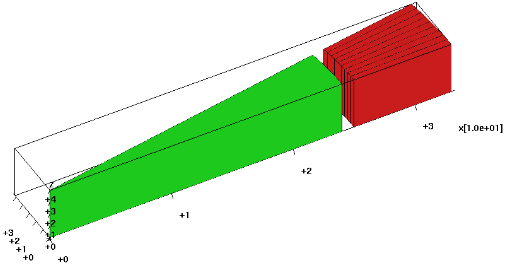

Parameters for simulation:

- Source current in induction coil $I_0 = 5000\ \mathrm{A}$ at $f = 100\ \mathrm{kHz}$
- Heating time $1.0\ \mathrm{s}$
- Nonlinear data for $\sigma, c_p, \rho, \kappa, \mu_r$
- Adaptive grid with approx. 50000 DOF

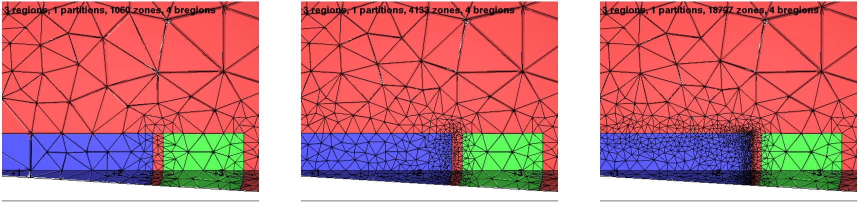

Figure: Adaptive grids

Example 1, HF: temperature and growth of austenite

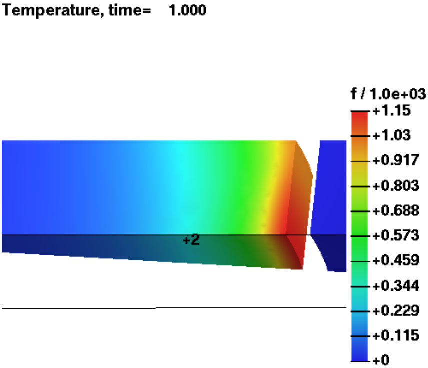

(Video: austenite.mp4)

Figure: temperature and austenite growth at high frequency

Example 1, HF: temperature and growth of austenite

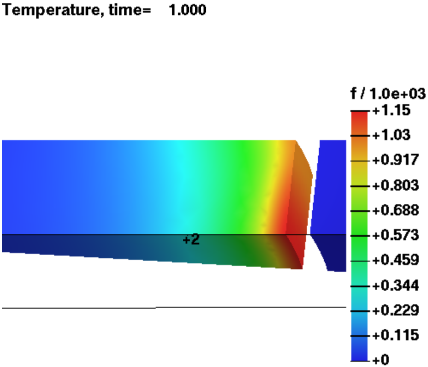

(Video: austenite.mp4)

Figure: temperature and austenite growth at high frequency

Example 1, HF vs. MF: Adaptive grid

- Source current in induction coil $I_0 = 5000\ \mathrm{A}$ at $f = 10\ \mathrm{kHz}$
- Heating time $1.0\ \mathrm{s}$
- Nonlinear data for $\sigma, c_p, \rho, \kappa, \mu_r$
- Adaptive grid with approx. 50000 DOF

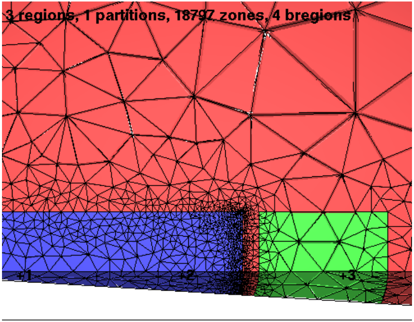

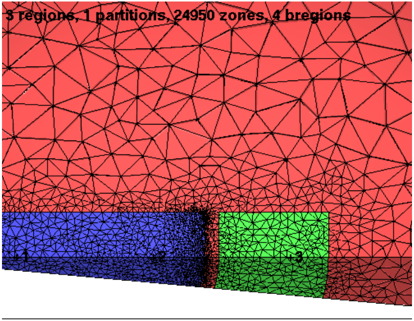

Figure: Comparison of the adaptive grid between HF (left) and MF (right)

Example 1, HF vs. MF: Temperature

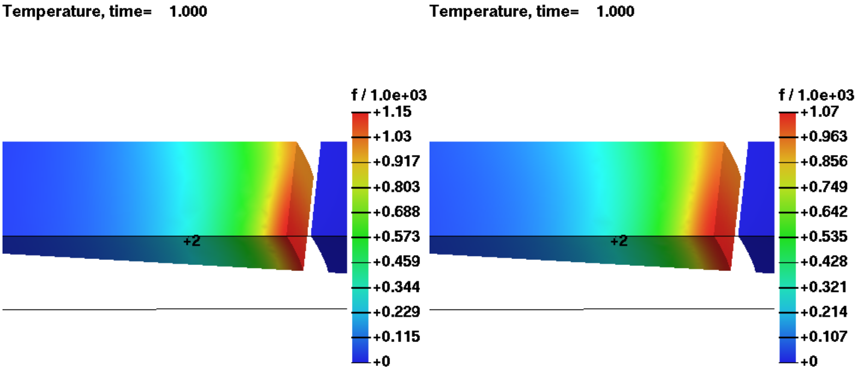

Figure: Comparison of the temperature profile after $1\mathrm{s}$ between HF (left) and MF (right)

Example 2

- Gear heated with HF and MF
- Adaptive grid
- Austenite profile
- Temperature profile

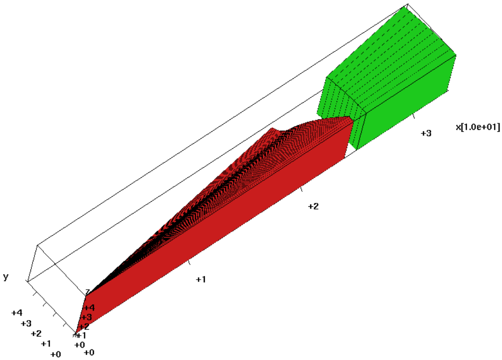

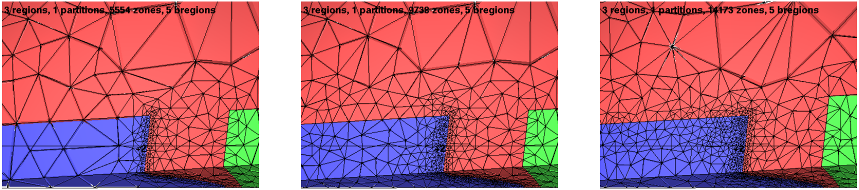

Figure: Adaptive grids

Example 2, HF: temperature

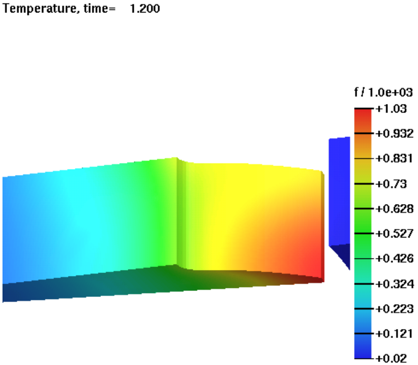

(Video: temperature.mp4)

Figure: temperature evolution at high frequency

Example 2, HF: temperature

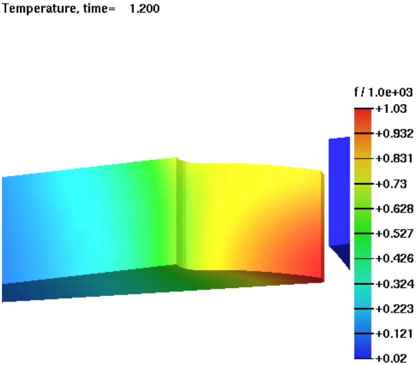

(Video: temperature.mp4)

Figure: temperature evolution at high frequency

Example 2, HF: growth of austenite

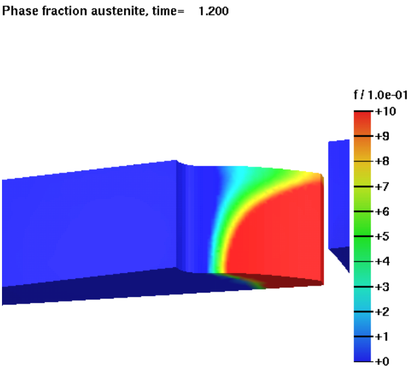

(Video: austenite.mp4)

Figure: austenite evolution at high frequency

Example 2, HF: growth of austenite

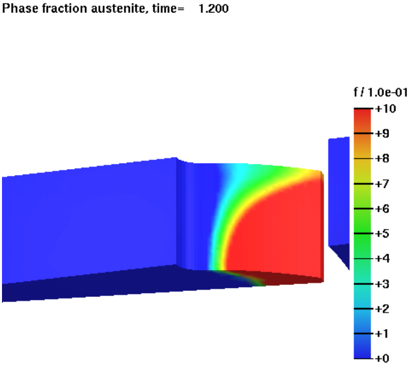

(Video: austenite.mp4)

Figure: austenite evolution at high frequency

Example 2, MF: temperature

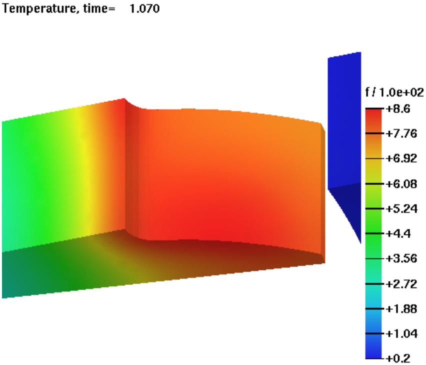

(Video: temperature.mp4)

Figure: temperature evolution at medium frequency

Example 2, MF: temperature

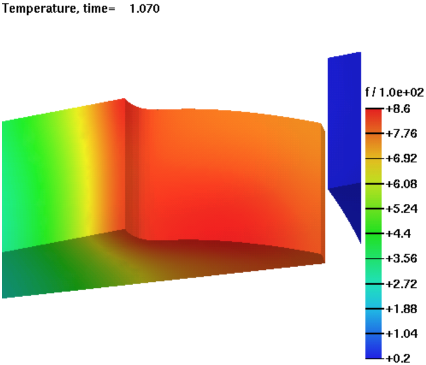

(Video: temperature.mp4)

Figure: temperature evolution at medium frequency

Example 2, MF: growth of austenite

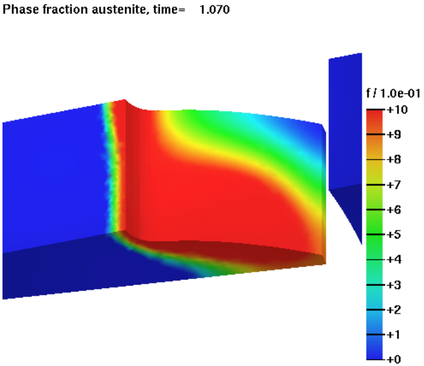

(Video: austenite.mp4)

Figure: austenite evolution at medium frequency

Example 2, MF: growth of austenite

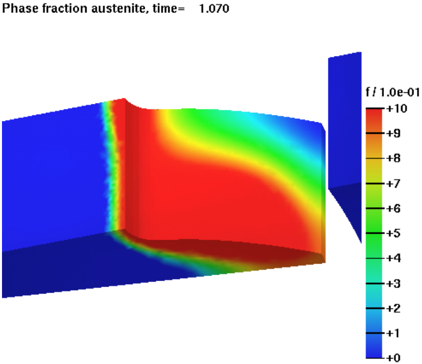

(Video: austenite.mp4)

Figure: austenite evolution at medium frequency

Comparison with experiments for disk shaped work piece

diameter [mm]	frequency [kHz]	inductor curr. [A]		simulation	Experiment		
		MF	HF	after 1 s	max. temp. nach 1 s	converter curr. [A]	
47,7	11,5	4800		1145	970-987	572-573	(9:1)
42	11,5	4800		678	687-700	573-575	
38,7	11,5	4800		553	537-550	572-575	
47,7	11,5	5157		1306			
42	11,5	5157		764			
38,7	11,5	5157		617			
47,7	200		1000	997	974-986	176-177	(10:1)
42	200		1000	725	711-716	176	
38,7	200		1000	610	601-658	176-177	
47,7	200		1100	1066			
42	200		1100	817			
38,7	200		1100	702			

- **Summary . . .**
  - modelling of multifrequency induction hardening
  - well-posedness of state system, derivation of optimality system
  - first results of numerical simulations

- **Summary ...**
  - modelling of multifrequency induction hardening
  - well-posedness of state system, derivation of optimality system
  - first results of numerical simulations

- **... and perspective**
  - add oscillator circuit model of machine
  - numerical optimal control
  - model reduction

- **Summary . . .**
  - modelling of multifrequency induction hardening
  - well-posedness of state system, derivation of optimality system
  - first results of numerical simulations

- **. . . and perspective**
  - add oscillator circuit model of machine
  - numerical optimal control
  - model reduction
  - industrial applications, e.g., helical gears

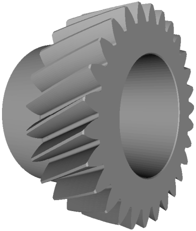

Thank you for your attention!

www.me-fre-sim.de

- Different crystal structures in iron

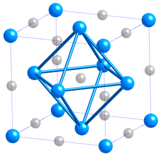

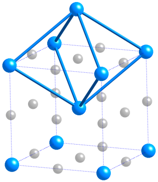

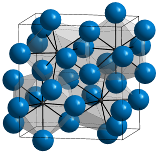

Austenite	Ferrite	Cementite
Face centered cubic (fcc)	Body centered cubic (bcc)	Orthorombic (Fe_3C)
Stable at high temperatures	Stable at low temperature	Metastable compound

- Different phases with different mechanical properties

Austenite: high temperature phase

Pearlite: lamellar mixture of ferrite and cementite
soft and ductile

Martensite: forms on rapid cooling
hard and brittle